Article

Viscosity and Structure of CaO-SiO2-FeO-MgO System During Modified Process from Nickel Slag by CaO

Yingying Shen*, Junkai Chong, Ziniu Huang, Jianke Tian, Wenjuan Zhang, Xingchang Tang, Wanwu Ding, Xueyan Du*

School of Materials & Science, State Key Laboratory of Advanced Processing and Recycling of Non-ferrous Metals, Lanzhou University of Technology, Lanzhou, 730050, China

* Correspondence: shenyingying005@163.com; duxy@lut.cn

Abstract: There is a high iron content in the nickel slag that mainly exists in fayalite phase. Basic Oxide can destroy the stable structure of fayalite which is beneficial to the treatment and comprehensive utilization of nickel slag. The reseach was based on the composition of the raw nickel slag, taking CaO-SiO2-FeO-MgO system as the object and CaO as a modifier. The effect of basicity on the melting characteristics, viscosity and structure of CaO-SiO2-FeO-MgO system was studied. The relationship between the viscosity and structure of CaO-SiO2-FeO-MgO system was also explored. The results show as follows. (1) When the basicity is lower than 0.90, the primary phase of the slag system is olivine phase. When the basicity is greater than 0.90, the primary phase of the slag system transform into monoxide. When the basicity is 0.90, olivine and monoxide precipitate together as the temperature continues to decrease. At the same time, the liquidus temperature, softening temperature, hemispherical temperature, and flow temperature all reach the lowest value. (2) With the increase of basicity, critical viscosity temperature of CaO-SiO2-FeO-MgO system decreases first and then increases. Critical viscosity temperature is the lowest at the basicity of 0.90, which is 1295 ℃. (3) When the slag system is heterogeneous, the viscosity of the molten slag increase rapidity because of the quantity of solid phase precipitated from CaO-SiO2-FeO-MgO system. (4) When the slag system is in a homogeneous liquid phase, the molar fraction of O^0 decreases with the increase of basicity and the mole fraction of O^- and O^{2-} increases continuously at the basicity of 0.38~1.50. The silicate network structure is gradually depolymerized into simple monomers, resulting in the degree of polymerization is reduced and the viscosity is reduced, too. The mole fraction of different kinds of oxygen atom is converged to a constant value when basicity is above 1.20.

Keywords: nickel slag; basicity; CaO-SiO2-FeO-MgO system; viscosity; structure

1. Introduction

Iron-rich nickel slag (Nickel slag) is the industrial waste discharged from the process of nickel metallurgy in flash furnace. The production of 1t nickel can produce about 6~16 t slag, and the emissions from Jinchuan Group Co. of Gansu Province in China is more than 1.6 million tons per year, with a cumulative stock of up to 40 million tons[1]. The content of TFe (total iron) in nickel slag is up to 40% and the valuable metal elements such as Ni, Co, and Cu also exist. Fayalite ($2FeO·SiO_2$) that as the main phase in the slag is a co-melt composed by complex silicates [2]. The structure of fayalite is stable, because it is a complex network crystal in which Si-O atom connected with each other, resulting in the low recovery of valuable metal from nickel slag[3]. Adding basic oxides can destroy the network structure of fayalite[4]. If an appropriate amount of CaO is added to the molten nickel slag, the decomposition of the fayalite can be promoted, which is beneficial to the further

43 reduction or oxidation treatment of the nickel slag in order to promote the comprehensive utilization
44 of the nickel slag[1, 5-6].

45   Viscosity is one of the typical physical properties of slag, which not only affects the chemical
46 reaction of slag, transfer rate of elements and precipitation of crystal, but also affects the life of
47 furnace liner. When the temperature of the slag is lower than the liquidus temperature, the quantity
48 and type of the phase has a significant influence on the viscosity of the slag system; and when the
49 temperature is higher than the liquidus temperature of the slag, the viscosity of the slag system is
50 mainly affected by the slag structure. The viscous performance of the slag is the macroscopic
51 performance of its microstructure. Many scholars have studied on the structure and viscosity of
52 different slag systems. Lv et al[7] studied the viscosity of SiO_2-MgO-FeO-CaO-Al_2O_3 slag system. The
53 results show that with the basicity increases, the degree of slag polymerization and the viscosity
54 both decreases. Talapaneni et al[8]combined experiments and theory to study the relationship
55 between melt structure and viscosity of high alumina silicates. The results show that the silicate
56 structure in the SiO_2-MgO-CaO-Al_2O_3 slag system was depolymerized with the increase of basicity,
57 resulting in the viscosity and activation energy of the slag are reduced.

58   There are more impurity elements exist, so the composition of nickel slag is complex. The
59 content of CaO, FeO, SiO_2 and MgO in nickel slag is as high as 94 wt%[9]. Therefore, nickel slag
60 system can be simplified to CaO-SiO_2-FeO-MgO system according to the composition. Based on the
61 composition of water-quenched nickel slag from enterprise flash furnace, this paper studied the
62 viscosity and structure of CaO-SiO_2-FeO-MgO system during modified process from nickel slag by
63 CaO, in order to provide a theoretical basis for modification of nickel slag.

64 **2. Experimental Procedure**

65 *2.1. Experimental Materials*

66   Experimental material; CaO(analytical reagent, Sinopharm Chemical Reagent Co., Ltd.),
67 SiO_2(analytical reagent, Sinopharm Chemical Reagent Co., Ltd.), MgO(analytical reagent,
68 Sinopharm Chemical Reagent Co., Ltd.), $FeC_2O_4 \cdot 2H_2O$(analytical reagent, Tianjin Guangfu Fine
69 Chemical Research Institute).

70   Pretreatment of raw materials; (1) Preparation of FeO by $FeC_2O_4 \cdot 2H_2O$. The powder of
71 $FeC_2O_4 \cdot 2H_2O$ was placed in a high-temperature tube furnace and heated to 1000 ℃ for 2 h under
72 300 mL/min of Ar protection. $FeC_2O_4 \cdot 2H_2O$ tends to break up into FeO, CO, CO_2 and H_2O[10-12]. After
73 cooling, The powder was ground to 200 mesh or less. (2) SiO_2, MgO, and CaO were dried in a
74 vacuum drying oven at 1000 ℃ for 2 h.

75 *2.2. Experimental Method*

76   According to the chemical composition of nickel slag, CaO-SiO_2-FeO-MgO system was taken as
77 the research object. The ternary basicity (basicity) of slag system was a variable, and the formula was
78 $R=(w$CaO$+w$MgO$)/w$$SiO_2$. The content of CaO, MgO, SiO_2 and FeO in raw nickel slag were 3.77%,
79 8.86%, 33.31%, 54.06% after the conversion of percentage, and the basicity was 0.38. In the
80 experiment, CaO was used as modifier. With the increase of the CaO content in the modified slag
81 system, the basicity was 0.60, 0.90, 1.20 and 1.50, respectively. The chemical composition of the
82 modified slag system designed was shown in Table 1.

83 **Table 1.** Chemical composition of modified slag system (wt%).

Slag System	CaO	MgO	SiO₂	FeO	Basicity
S1	3.77	8.86	33.31	54.06	0.38

S2	10.36	8.26	31.03	50.35	0.60
S3	17.99	7.75	28.39	46.07	0.90
S4	24.43	6.96	26.15	42.46	1.20
S5	29.93	6.45	24.25	39.37	1.50

84   2.2.1. Preparation of pre-melted slag sample

85   The preparation steps of pre-melting slag sample were as follows: (1) The pre-treated chemical
86   reagent was weighed according to the data in Table 1, and then put in a mortar for 30 minutes to
87   make the composition mixed uniformly. (2) The uniform chemical reagent was pressed into a
88   cylinder with the diameter of 30 mm and the height of 10 mm under the pressure of 20 MPa. Then
89   placed it into a corundum crucible; (3) The crucible containing the sample was put into the
90   High-temperature Tube Furnace with the temperature raised to 1550 ℃ at a heating rate of 3 ℃
91   /min. After 2 h of heat preservation, it was cooled to room temperature at a cooling rate of 3 ℃/min.
92   Throughout the process, 300 mL/min of Ar was used as the protecting gas. (4) The pre-melted slag
93   was crushed to 200 mesh (0.074 mm).

94   2.2.2. Determination of characteristic temperature

95   The characteristic temperature was measured by LZ-III Slag Melting Temperature
96   Characteristic Tester shown as Figure 1. The experimental method was as follows: 1) Weigh 10g of
97   pre-slag and press the sample with a sample mold. The sample was a cylinder with the diameter of 3
98   mm and the height of 3 mm. 2) The prepared sample was placed in the LZ-III Slag Melting
99   Temperature Characteristic Tester. 3) With the temperature increased at the rate of 5℃/min, the
100   corresponding temperature was recorded as the softening temperature, hemisphere temperature
101   and flow temperature when the sample dropped to 75%, 50%, and 25%, respectively[13,14].
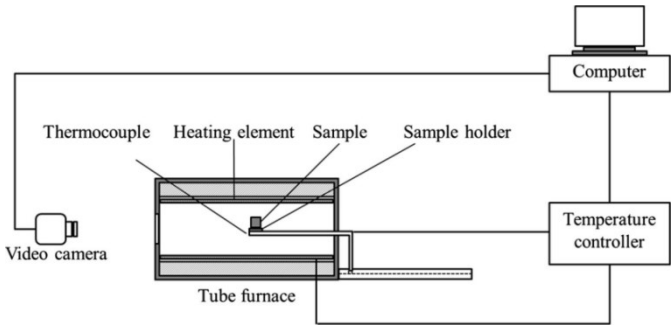102   Throughout the process, 300 mL/min of Ar was used as the protecting gas.

103

104   **Figure 1.** Diagram of LZ-III Slag Melting Temperature Characteristic Tester

105   The characteristic temperature points to be observed were as follows: 1) softening temperature,
106   the temperature at which the sample had fused down to a spherical lump in which the height was
107   75% of original sample. 2) hemisphere temperature, the temperature at which the sample had fused
108   down to a hemisphere lump in which the height was 50% of original sample. 3) flow temperature,
109   the temperature at which the fused mass had spread out in a nearly flat layer with a maximum
110   height of 25% of the of original sample. Figure 2 was shown the height changes of slag melting
111   process. These three temperatures characterize the melting trajectory of flux in industrial
112   applications. The hemispherical temperature is referred to as the melting temperature of the mold
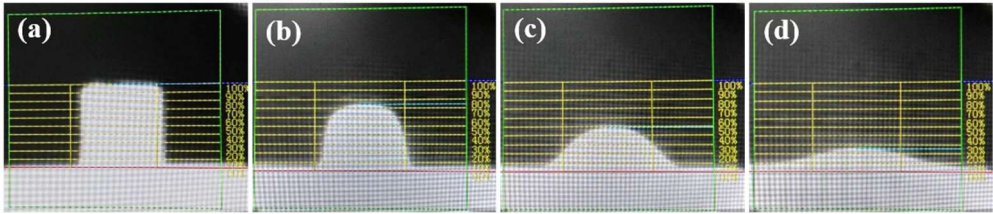113   flux[13, 15].

114

115   **Figure 2.** The height changes of slag melting process

116   (a) the original height   (b) the corresponding height of softening temperature

117 (c) the corresponding height of hemspheric temperature   (d) the corresponding height of flow temperature

118

119   2.2.3. Measurement of the viscosity

120

121   **Figure 3.** Experimental apparatus of viscosity measurements

122 The experimental apparatus of viscosity measurements was shown in Figure 3[16]. This technique
123 was widely used due to its relative simplicity and reproducibility. The experiments were conducted
124 in a corindon reaction tube using a Kanthal Super electrical resistance furnace. A B-type
125 thermocouple and a Proportional Integral Differential control system were used to maintain the
126 target temperature. The experimental method was as follows[17]: 1) Weigh 130g of pre-slag and press
127 into a cylinder with the diameter of 30 mm and the height of 10 mm at a pressure of 20 MPa using a
128 tableting machine. 2) Then place it in a corundum crucible with the diameter of 40 mm and the
129 height of 120 mm. 3) 1.5 L/min of the high purity argon gas was injected into the tube to control the
130 atmospheric conditions. The gases were passed through soda lime to remove excess moisture. 4)
131 Place the crucible into the RTW-16 High Temperature Melt Property Tester in the hot zone of the
132 furnace and the temperature of the hot zone was controlled to 1500℃ and was maintained for 1 h to
133 achieve thermal equilibrium of the slag. 5) During the cooling process, the slag viscosity was
134 measured by the rotational torque method. After the spindle was placed in the slag, the viscosity
135 was measured by lowering the temperature by 50 ℃ over a period of 10 min and maintaining the
136 temperature for about 30 min for the viscosity measurement. The rotational speed of the spindle was
137 fed back to the computer. It should be noted that, because the pure Ar gas was blown, the low
138 oxygen partial pressure was maintained and most of Fe would be present as Fe^{2+}. The temperature
139 was calibrated before each experiment using a B-type thermocouple inserted from the top of the
140 reaction tube. The castor oil was used as the material to calibration before the viscosity
141 measurements.

142   2.2.4. Preparation of water quenching slag sample

143   10g of pre-melted slag was weighed and put into a corundum crucible. Then place it into the
144 Vertical Quenching Furnace and heat it to 1500 ℃ at the rate of 3 ℃/min. After holding for 2 h, the
145 molten slag was quenched by water. Throughout the process, 300 mL/min of Ar was used as the
146 protecting gas. The water-quenched slag sample was dried in a vacuum oven for 10 h, then crushed
147 and sieved to 200 mesh (0.074 mm). The microstructure was analyzed by FT-IR and XPS.

148 *2.3. Calculation Method by FactSage.*

149   In this paper, the influence of basicity on the phase diagram of CaO-SiO$_2$-FeO-MgO system was
150 calculated by the module of Phase Diagrm in FactSage7.1 thermodynamic software. The
151 precipitation of the phase in the slag system during non-equilibrium solidification under different
152 basicity was calculated by the module of Equilib.

153 **3. Results and Discussion**

154 *3.1. Effect of Basicity on Melting Characteristics of CaO-SiO$_2$-FeO-MgO System*
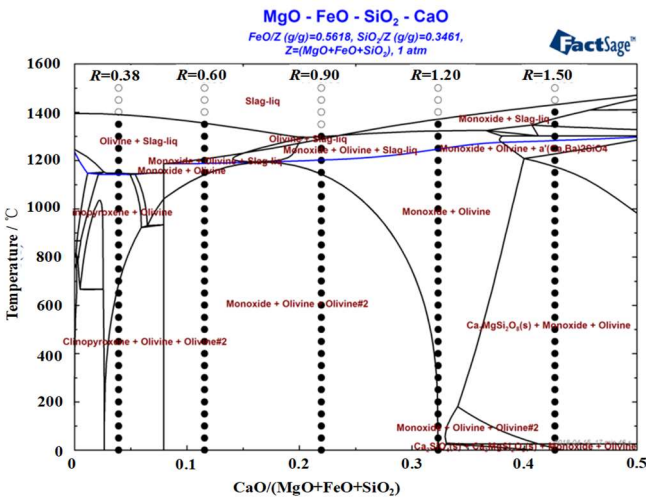

156 **Figure 4.** Phase diagram of CaO-SiO$_2$-FeO-MgO slag system in argon atmosphere

157   Figure 4 shows the phase diagram of CaO-SiO$_2$-FeO-MgO slag system in argon atmosphere.
158 The totle mass of MgO, FeO and SiO$_2$ marked 'Z', thus, FeO/Z and SiO$_2$/Z was 0.5618 and 0.3461 in
159 the system. Temperature versus CaO/Z was shown in Figure 2. It can be seen from figure that when
160 the basicity is lower than 0.90, the primary phase of the slag system is olivine phase. When the
161 basicity is greater than 0.90, the primary phase of the slag system transform into monoxide. With
162 the basicity increased, the area of the olivine phase gradually decreases, and the liquidus
163 temperature decreases first and then increases. When the basicity is 0.90, the liquidus temperature
164 is about 1297 ℃ and reaches the lowest, olivine and monoxide precipitate together as the
165 temperature continues to decrease.

166   Figure 5 shows the effect of basicity on the characteristic temperature of CaO-SiO$_2$-FeO-MgO
167 system. It can be seen from the figure that when the basicity is 0.38~1.50, the softening temperature,
168 hemisphere temperature and flow temperature of the slag system decrease first and then increase
169 with the increase of basicity. When the basicity is 0.90, the softening temperature, hemisphere
170 temperature and flow temperature are all the lowest, which are 1244 ℃, 1256 ℃ and 1274 ℃. The
171 reason is analyzed as follows. When the basicity is 0.38~0.90, with the increase of basicity, CaO
172 destroys the network structure of olivine phase, resulting in the olivine phase gradually
173 disintegrates[18,19]. The effect of CaO is obvious that conducive to the lowering of the liquidus
174 temperature of the slag system, as the softening temperature, hemisphere temperature and flow
175 temperature are also reduced. When the basicity is 0.90~1.50, CaO itself has a high melting point and

176   is easy to combine with other components in the slag system to form the high melting point
177   substance, so that the liquidus temperature, softening temperature, hemispherical temperature and
178   flow temperature of the system are gradually increased. The flow temperature is significantly higher
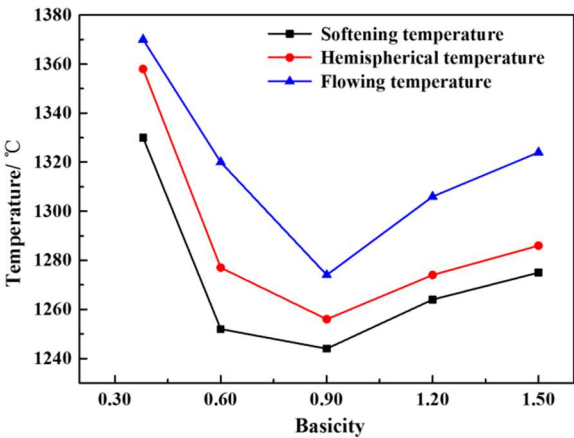179   than the softening temperature and the hemispherical temperature, resulting in the deterioration of
180   fluidity.

181

182   **Figure 5.** Effect of basicity on characteristic temperature of CaO-SiO$_2$-FeO-MgO system.

183   *3.2. Effect of Basicity on the Viscosity of CaO-SiO$_2$-FeO-MgO system*

184   3.2.1. Effect of basicity on viscosity-temperature curve of CaO-SiO$_2$-FeO-MgO system

185
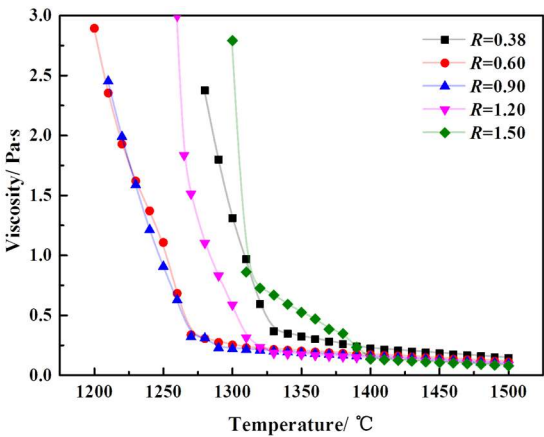
186   **Figure 6.** Viscosity-temperature curve of CaO-SiO$_2$-FeO-MgO system at different basicity.
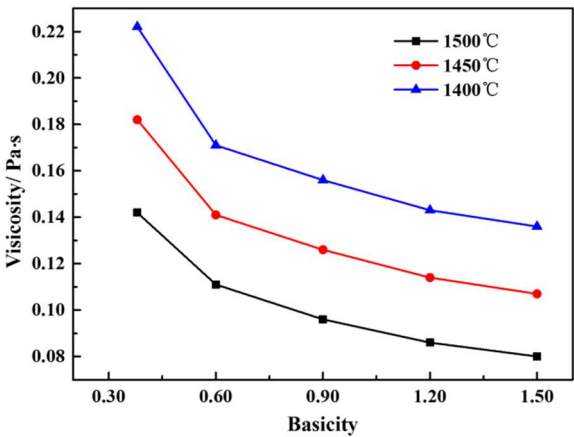

187

188   **Figure 7.** Curve between basicity and viscosity of slag at different temperature.

189 Figure 6 shows the viscosity-temperature curve of CaO-SiO$_2$-FeO-MgO system at different
190 basicity. It can be seen from the figure that the viscosity of the slag system is all lower than 0.25 Pa·s
191 when the temperature is higher than 1400℃, with the basicity is in the range of 0.38~1.50. At the
192 same basicity condition, the temperature decreases, the viscosity change of the slag system is not
193 significant. The reason is analyzed as follows. When the basicity is 0.90, the liquidus temperature of
194 the modified slag system is the lowest, which is 1297 ℃. When the basicity is 1.50, the liquidus
195 temperature of the modified slag system is the highest, which is 1394 ℃. When the temperature is
196 above the liquidus temperature, the slag is a homogeneous system. And the temperature is below
197 the liquidus temperature, the slag is a heterogeneous system[20]. When the temperature is higher than
198 1400 ℃, the slag system is in a uniform liquid phase at the range of 0.38~1.50. The microstructure of
199 the slag plays a leading role in the viscosity of the slag system. The effect of the slag microstructure
200 on the slag viscosity is weak, resulting in the less change in viscosity. When the temperature is lower
201 than 1400 ℃, the system is a heterogeneous slag system. As the decrease of temperature, the
202 viscosity of the slag system with different basicity at different temperatures is mainly related to the
203 type and quantity of the precipitate phase from the slag system. At the same time, when the viscosity
204 of slag is higher than 0.25 Pa·s, it increases rapidly with the decrease of temperature, which has the
205 characteristic of typical crystallization slag at the basicity of 0.38, 0.60, 0.90,1.20. When the viscosity is
206 higher than 0.75 Pa·s, viscosity of the slag begins to rise sharply with the temperature decreases and
207 has typical plastic slag characteristics at the basicity of 1.50, because of the high basicity.

208 Figure 7 shows the effect of basicity on the viscosity of CaO-SiO$_2$-FeO-MgO system at different
209 temperatures. It can be seen from the figure that the viscosity of the slag system gradually decreases
210 with the increase of basicity when the slags are all above the liquidus temperature (1400~1500℃). At
211 the same basicity, the viscosity of the slag is gradually reduced with the increase of temperature. At
212 1500℃, when the basicity increases from 0.38 to 0.60, the viscosity decreases rapidly from 0.14 Pa·s to
213 0.11 Pa·s. When the basicity increases from 0.60 to 1.50, the viscosity decreases slowly from 0.11 Pa·s
214 to 0.08 Pa·s. With the increase of basicity, the trend of viscosity reduction is consistent when the
215 temperature is in the range of 1400~1500 ℃.

216 3.2.2. Effect of Basicity on Critical Viscosity Temperature of CaO-SiO$_2$-FeO-MgO System

217 As the slag is gradually cooled from the liquid phase, the viscosity gradually increases. When
218 the temperature drops to a certain point, the viscosity will increase rapidly, This temperature point
219 is called critical viscosity temperature (T_{cv})[21]. It is well known that viscosity measurements taken at
220 temperatures higher than the critical viscosity temperature to be those in the fully liquid region of
221 the system. To highlight the critical viscosity temperature and the experimental test region, the
222 viscosity as a function of temperature in the CaO-SiO$_2$-FeO-MgO system at the basicity of 0.38 is
223 given as an example in Figure 8. The critical viscosity temperature is known as the temperature at
224 which the slope changes in the Arrhenius plot (ln(viscosity)-1/T graph). The natural logarithm of
225 viscosity as a function of reciprocal temperature shows a significant increase below temperatures of
226 1380 ℃(1653K), which is the solid-liquid coexisting region, and it suggests the formation of solid
227 precipitates[22]. Thus, the experimental measurements were taken above the critical viscosity
228 temperature as described by Figure 8. By the same way, at the basicity of 0.60, 0.90, 1.20, 1.50, critical
229 viscosity temperatures are 1360℃, 1295℃, 1372℃ and 1393℃, respectively.

230 Figure 9 shows the effect of basicity on critical viscosity temperature of CaO-SiO$_2$-FeO-MgO
231 system. It can be seen that critical viscosity temperature of the slag system decreases firstly and then
232 increased with the increase of basicity at the range of 0.38~1.50. And critical viscosity temperature is
233 the lowest which is 1295℃ at the basicity of 0.90. In order to ensure the migration of components in
234 the slag and strengthen the dynamic conditions of the reaction, the lower viscosity and good fluidity
235 of the slag system at the smelting temperature range is beneficial to the process of metallurgical
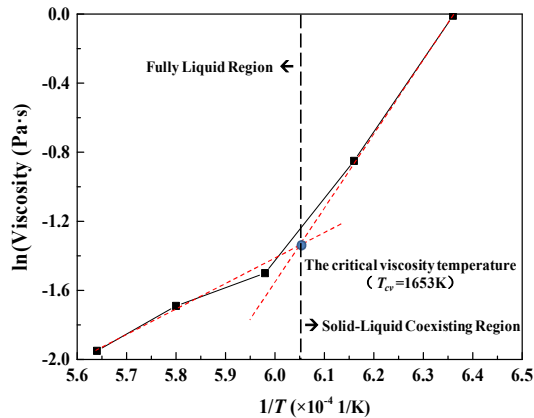236 production. So it is necessary to reduce critical viscosity temperature of the slag system.

237

238 **Figure 8**. Example of the critical viscosity temperature for the CaO-SiO$_2$- FeO-MgO system at the
239 basicity of 0.38. Note the critical viscosity temperature is 1380 ℃(1653K).
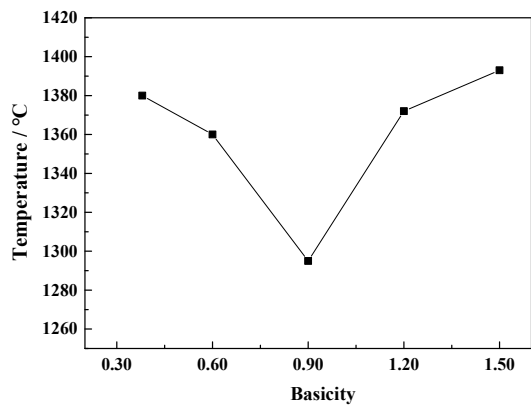
240

241 **Figure 9.** Relationship between basicity and critical viscosity temperature of CaO-SiO$_2$-FeO-MgO
242 system.

243 3.2.3. Effect of Phase Precipitation on the Viscosity of CaO-SiO$_2$-FeO-MgO System

244 Figure 10 is the XRD patterns of CaO-SiO$_2$-FeO-MgO system by water quenching at 1290℃. It
245 can be seen from figure that the primary crystal phase precipitated of the slag system is
246 FeO(monoxide) when the basicity is 1.50 and (Mg,Fe)$_2$SiO$_4$(olivine) when the basicity is 0.38. At the
247 basicity of 0.90, FeO and (Mg,Fe)$_2$SiO$_4$ exist simultaneously. The experimental result is in agreement
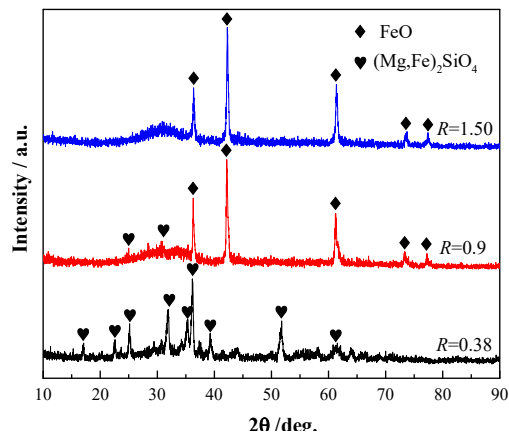248 with the phase diagram analysis results.

249

250 Figure. 10. XRD spectrum of CaO-SiO$_2$-FeO-MgO system

251   Figure 11 shows the effect of solid precipitation in modified slag system on viscosity of the slag.

252 Because the viscosity of the slag is affected by the contents of solid phase and liquid phase at high

253 temperature, and the former is more significant[23]. When the slag system continues to cool below the

254 liquidus temperature, the solid phase can be precipitated because of the saturation as the

255 temperature decreases and continue to be formed. At this time, the viscosity of the slag will increase

256 rapidly. The formation rate of solid phase is smaller when the temperature is higher than critical

257 viscosity temperature of the slag system. By contrast, the formation rate of solid phase is

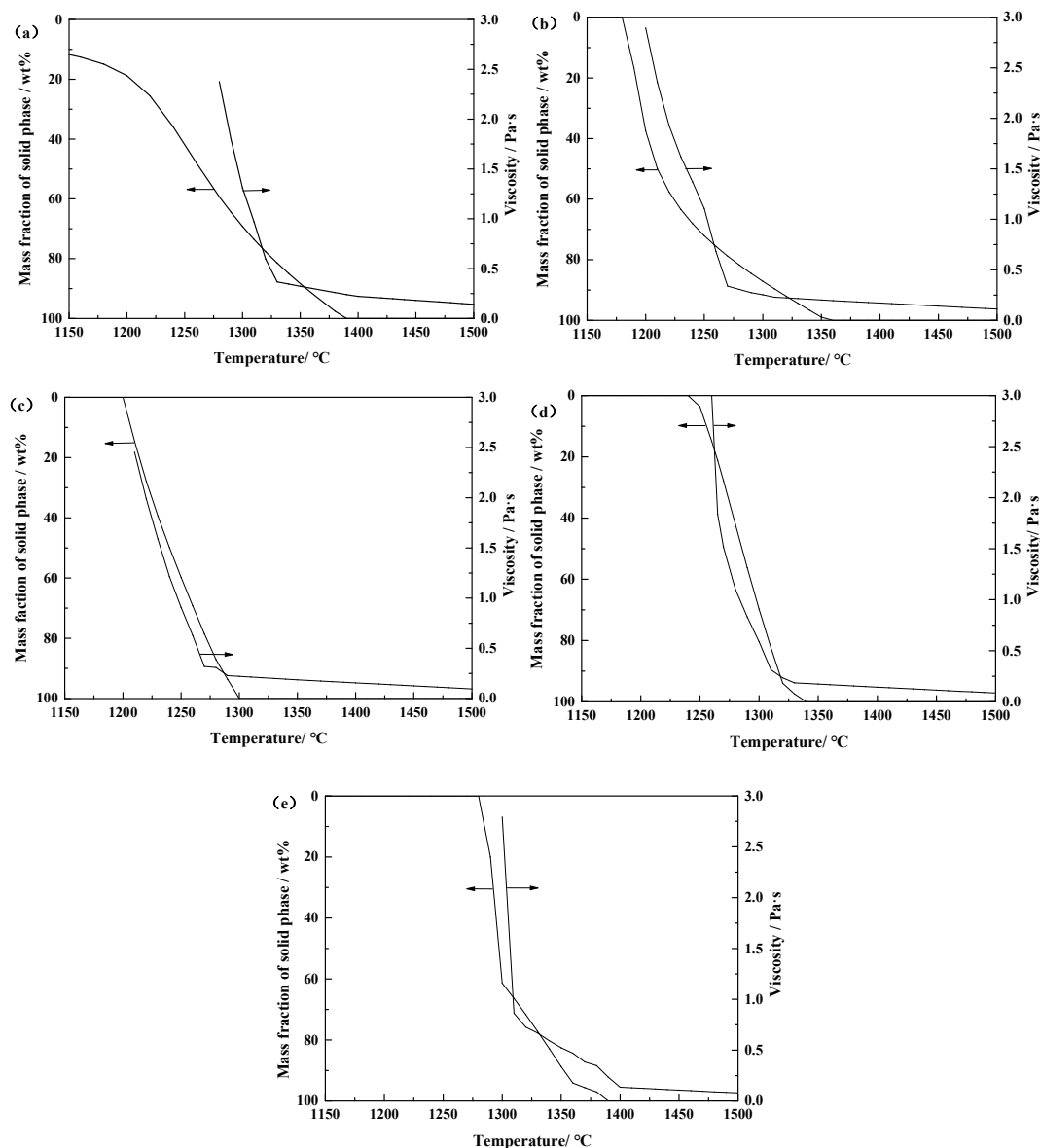258 significantly increased when the temperature is lower than critical viscosity temperature.

259

260

261

262   **Figure 11.** Effect of solid phase precipitation on the viscosity of CaO-SiO$_2$-FeO-MgO system at
263   different basicity: (a) *R*=0.38；(b) *R*=0.60；(c) *R*=0.90；(d) *R*=1.20；(e) *R*=1.50.

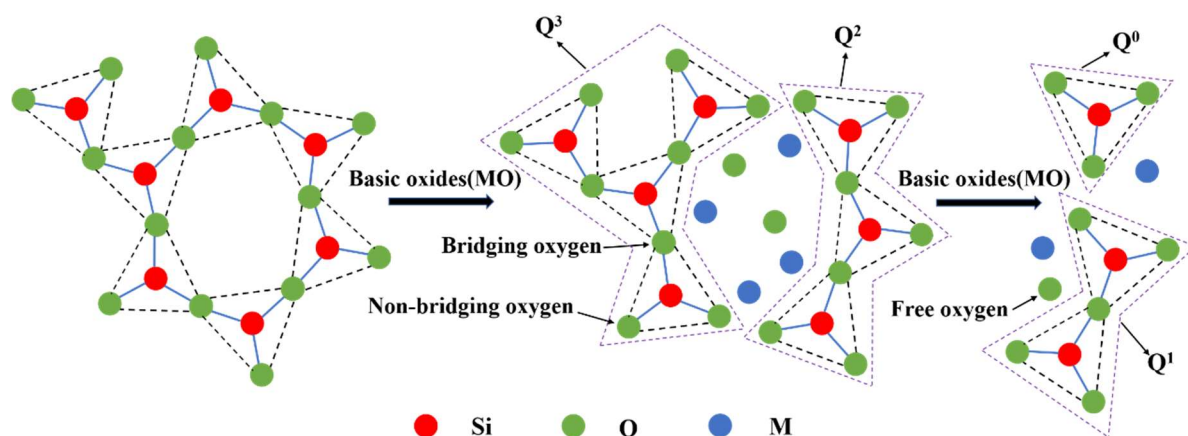264 *3.3. Effect of Basicity on the Structure of CaO-SiO$_2$-FeO-MgO System*

**Figure 12.** Schematic disintegration of silicate structure by basic oxides.

Figure 12 shows the schematic disintegration of the silicate structure by basic oxides. There are three types of oxygen in the molten slag, as shown as follows[24]. 1) Bridging oxygen (O^0, the oxygen atom is connected to two silicon atom). 2) Non-bridging oxygen (O^-, the oxygen atom is connected to a silicon atom). 3) Free oxygen (O^{2-}, the oxygen atom is not connected to the silicon atom). With the addition of basic oxides, free oxygen will enter the silicate system and destroy the bridge oxygen bonding in the silicate structure. Thereby the complicated silicate network structure becomes a simple silicate structure and a large number of non-bridged oxygen forms. For example, the main structure of $[Si_3O_9]^{6-}$ combines with the free oxygen released by the basic oxide to decompose into a dimeric structure of $[Si_2O_7]^{6-}$ and a monomeric structure unit of $[SiO_4]^{4-}$, while the cation of the basic oxide will act as a balancing charge. Q^3, Q^2, Q^1, and Q^0 indicate that the number of bridge oxygens connected to each silicon atom is 3, 2, 1, and 0.

Figure 13 shows the FT-IR spectra of water quenching slag sample at 1500°C. $[SiO_4]^{4-}$ tetrahedron symmetric stretching vibration zone in the range of 800~1200 cm^{-1}, the four kinds of Si-O zones in 1100~1150 cm^{-1} (Q^3, layered), 950~980 cm^{-1} (Q^2, chain), 900~920 cm^{-1} (Q^1, dimer), 850~880 cm^{-1} (Q^0, monomer)[25, 26]. It can be seen from the figure that as the basicity increases from 0.38 to 1.50, the center position of the $[SiO_4]^{4-}$ tetrahedral symmetric stretching vibration zone gradually shifts to the low wavenumber region and the valley depth of the [Si-O] bending vibration zone is gradually reduced. At the same time, the valley depth corresponding to the central position of Q^0 is gradually deepened and the valley depth corresponding to the central position of Q^3 is gradually shallower, but the valley depth corresponding to the central position of Q^1 and Q^2 is not obvious. It indicates that CaO as a network modification gradually destroy the complex network structure of silicate into a simple dimer (Q^1) or monomer (Q^0), which leads to the continuous decrease of the polymerization degree of silicate.
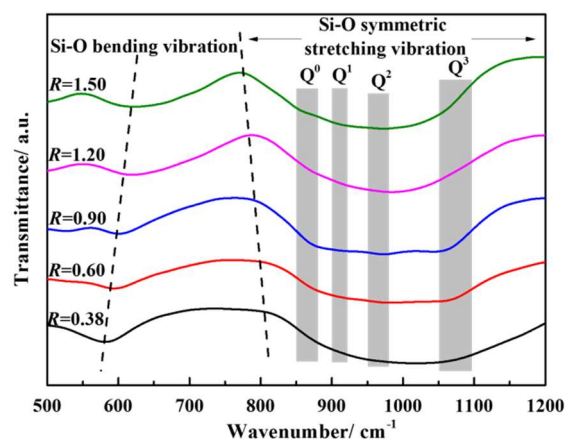
291   **Figure 13.** FT-IR spectra of water quenching slag sample.

292
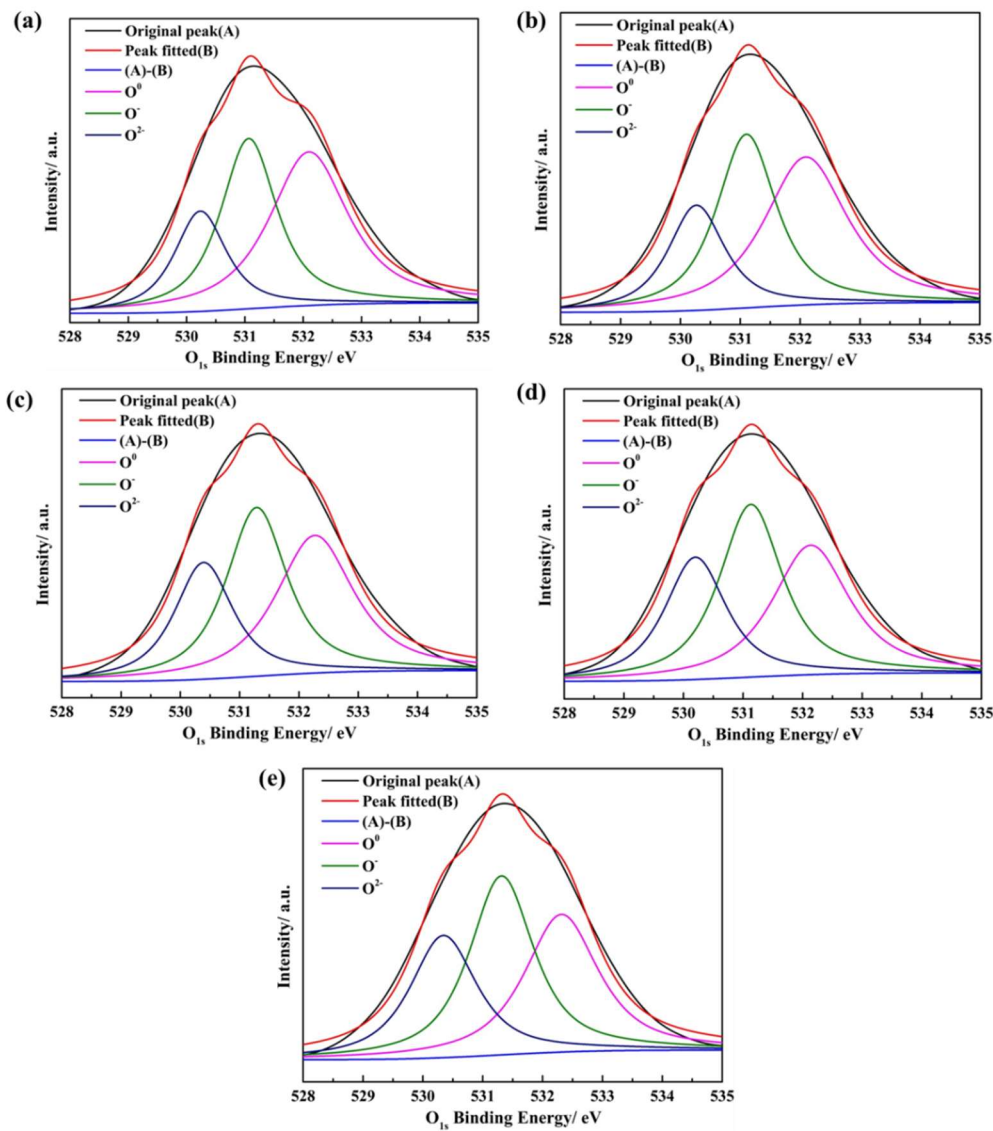
293   **Figure 14.** XPS peak fitting spectrum of O_{1s} in water quenching slag sample at different basicity：(a)
294   *R*=0.38；(b) *R*=0.60；(c) *R*=0.90；(d) *R*=1.20；(e) *R*=1.50.

295   **Table 2.** Fitting positions and mole fractions of different types of oxygen atom.

basicity	O^0		O^-		O^{2-}	
	position (eV)	Mole fraction	position (eV)	Mole fraction	position (eV)	Mole fraction
R=0.38	532.10	45.01%	531.07	35.48%	530.24	19.51%
R=0.60	532.09	42.94%	531.10	36.25%	530.27	20.81%
R=0.90	532.27	38.46%	531.29	36.94%	530.39	24.60%
R=1.20	532.14	35.16%	531.13	38.24%	530.20	26.60%
R=1.50	532.31	34.12%	531.31	38.56%	530.34	27.31%

296　　　　The peak of O_{1s} in the XPS spectrum can be decomposed into the peaks corresponding to
297　three different kinds of oxygen atom. For the different basicity from 0.38 to 1.50, the accuracy (r^2) of
298　deconvolution of XPS peak is 21.78, 22.13, 23.32, 24.97 and 27.73, respectively. The XPS peak was
299　calibrated through Au calibration[27, 28]. The envelope of the O_{1s} peak of the water quenching slag
300　samples at different basicity is divided by the Gaussian function. The distribution information of the
301　characteristic peaks in this region is shown in Figure 14. The ratio of the integral area of the peak
302　corresponding to different kinds of oxygen atom to the integral area of the O_{1s} peak is the mole
303　fraction. The positions and mole fractions of O^0, O^-, O^{2-} at different basicity are shown in Table. 2.
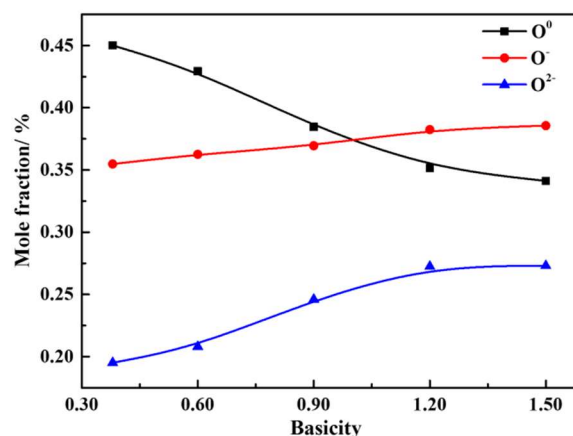
304

305　　　　　　**Figure 15.** Curve of the mole fraction of different kinds of oxygen atom with the basicity.

306　　　　Figure 15 shows the effect of basicity on the mole fraction of different oxygen atom in
307　CaO-SiO$_2$-FeO-MgO water-quenched slag samples. It can be seen from the figure that when the
308　range of the basicity is 0.38~1.50, the molar fraction of O^0 decreases with the increase of basicity, and
309　the mole fraction of O^- and O^{2-} increases continuously. The molar fractions of O^0, O^- and O^{2-} changed
310　significantly at the basicity of 0.38~1.20. But the molar fractions of O^0, O^- and O^{2-} are almost
311　unchanged when the basicity continues to increase to 1.50. It is shown that with the increase of
312　basicity, the silicate network structure is gradually depolymerized into simple monomers, resulting
313　in the degree of polymerization is reduced and the viscosity is gradually reduced, which is
314　consistent with the results of FT-IR spectra analysis. At the same time, it also explains the reason of
315　the viscosity decreases gradually with the increased basicity in Figure 7 from the level of
316　microstructure.

317　　　　Equation 1 is a fundamental result of the charge balance required by the tetrahedral

318　co-ordination of oxygen with silicon, and when any silicate anions associate to form higher polymers

319　plus oxygen ions, the overall reaction reduces to equation 1.

320
$$2O^- \rightarrow O^0 + O^{2-} \tag{1}$$

321　　　　Under equilibrium conditions, an equilibrium constant k may be written according to

322　Equation 2[29]. The curve of k with basicity of the CaO-SiO$_2$-FeO-MgO system is as shown in Figure

323　16. It can be seen from the figure that the mole fraction of different kinds of oxygen atom is

324　converged to a constant value when basicity is above 1.20.
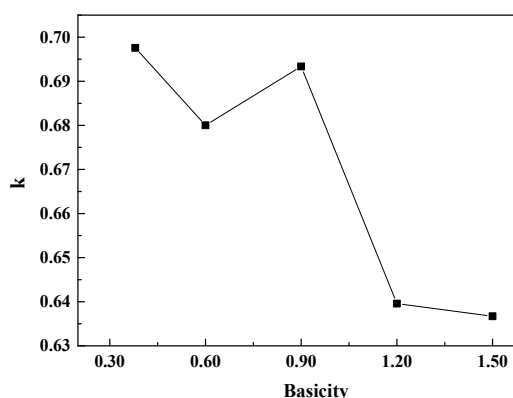
325
$$k = \frac{(O^0)\ (O^{2-})}{(O^-)^2} \tag{2}$$

326

Figure 16. The curve of k with basicity of the CaO-SiO$_2$-FeO-MgO system

328

4. Conclusion

The viscosity and structure of CaO-SiO$_2$-FeO-MgO system during modified process from nickel slag by CaO at the basicity of 0.38~1.50 is systematically studied in this paper. The results show as follows.

(1) When the basicity is lower than 0.90, the primary phase of the slag system is olivine phase. When the basicity is greater than 0.90, the primary phase of the slag system transform into monoxide.When the basicity is 0.90, olivine and monoxide precipitate together as the temperature continues to decrease. At the same time, the liquidus temperature, softening temperature, hemispherical temperature, and flow temperature all reach the lowest value.

(2) With the increase of basicity, critical viscosity temperature of CaO-SiO$_2$-FeO-MgO system decreases first and then increases. Critical viscosity temperature is the lowest at the basicity of 0.90, which is 1295 ℃.

(3) When the slag system is heterogeneous, the viscosity of the molten slag increase rapidity because of the quantity of solid phase precipitated from CaO-SiO$_2$-FeO-MgO system.

(4) When the slag system is in a homogeneous liquid phase, the molar fraction of O^0 decreases with the increase of basicity and the mole fraction of O^- and O^{2-} increases continuously at the basicity of 0.38~1.50. The silicate network structure is gradually depolymerized into simple monomers, resulting in the degree of polymerization is reduced and the viscosity is reduced, too. The mole fraction of different kinds of oxygen atom is converged to a constant value when basicity is above 1.20.

Author Contributions: Author Contributions: Conceptualization, Y.S. and X.D.; Methodology, Y.S. and X.D.; Software, J.C. and Z.H; Validation, Y.S. and X.D.; Formal Analysis, J.C.; Investigation, J.C., Z.H., and J.T.; Resources, X.D.; Data Curation, J.C. and Z.H.; Writing—Original Draft Preparation, J.C.; Writing—Review and Editing, X.D., and Y.S; Visualization, J.C. and Z.H.; Supervision, X.D., W.Z. and X.T.; Project Administration, Y.S.; Funding Acquisition, X.D., Y.S. and W.D.

Conflicts of Interest: The authors declare no conflict of interest.

References

1. Ni, W.; Jia, Y.; Zheng, F.; Wang, Z.J.; Zheng, M.J. Comprehensive utilization of iron recovery from Jinchuan nickel residue [J], Chinese Journal of Engineering, 2010, 32(8): 975-980.

2. Zhao, J.X.; Zhao, Z.Y.; Cui, Y.R.; Shi, R.M.; Tang, W.D.; Li, X.M.; Shang, N. New slag for nickel matte smelting process and subsequent Fe extraction[J]. Metallurgical and Materials Transactions B, 2018, 49(1): 304-310.

3. Ni, W.; Ma, M.S.; Wang, Y. L.; Wang, Z.J.; Liu, F.M. Thermodynamic and kinetic in recovery of iron from nickel residue[J]. Journal of University of Science and Technology Beijing, 2009, 31(2)：163-168.

4. Wang, Z.J.; Ni, W.; Jia, Y.; Zhu, L.P.; Huang, X.Y. Crystallization behavior of glass ceramics prepared from the mixture of nickel slag, blast furnace slag and quartz sand[J]. Journal of Non-Crystalline Solids, 2010, 356(31): 1554-1558.

5. Lv, F.L. Direct Reduction and Magnetic Separating Experiment Study of Nickel Slag [J]. Jiugang Technology, 2014, (3)：1-6+11.

6. Shen, Y.Y.; Chen, M.; Zhang, Y.Y.; Xu, X.Q. Li, G.Z.; Du, X.Y. Influence of temperature control system on the crystallisation behavior of magnetite phases in nickel Slags[J], Steel Research International, 2018, 89(3): 1700300.

7. Lv, X.M.; Lv, X.W.; Wang, L.W.; Qiu, J., Liu, M. Viscosity and structure evolution of the SiO_2-MgO-FeO-CaO-Al_2O_3 slag in ferronickel smelting process from laterite[J]. Journal of Mining & Metallurgy, 2017, 53(2): 147-154.

8. Talapaneni, T.; Yedla, N.; Pal, S.; Sarkar, S. Experimental and Theoretical Studies on the Viscosity-Structure Correlation for High Alumina-Silicate Melts[J]. Metallurgical & Materials Transactions B, 2017, 48(3): 1450-1462.

9. Shen, Y.Y.; Huang, Z.N.; Zhang, Y.Y.; Zhong, J.K.; Zhang. W.J.; Yang, Y.; Chen, M.;Du, X.Y. Transfer behavior of Fe element in nickel slag during molten oxidation and magnetic separation processes[J]. Materials Transactions, 2018, 59(10): 1659-1664.

10. Gao, Y.; Duan, C.; Yang, Y. Effect of applied voltage on electroreduction with controlled oxygen flow of molten slag containing FeO at 1723 K[J]. ISIJ International, 2015, 55(11): 2273-2282.

11. Gao, Y.M.; Wang, B.; Wang, S.B. Study on electrolytic reduction with controlled oxygen flow for iron from molten oxide slag containing FeO[J]. Journal of Mining & Metallurgy B: Metallurgy, 2013, 49(1): 49-55.

12. Sun, C.Y.; Guo, X.M. Electrical conductivity of MO (MO=FeO, NiO)-containing CaO-MgO-SiO_2-Al_2O_3 slag with low basicity[J]. Transactions of Nonferrous Metals Society of China, 2011, 21(7): 1648-1654.

13. Wang, L.; Zhang, C.; Cai, D.; Zhang, J.; Sasaki, Y.; Ostovski, O. Effects of CaO/SiO_2 ratio and Na_2O content on melting properties and viscosity of SiO_2-CaO-Al_2O_3-B_2O_3-Na_2O mold fluxes[J]. Metallurgical & Materials Transactions B, 2017, 48(1) : 516-526.

14. Xu, J.F.; Zhang, J.Y.; Jie, C.; Tang, L.; Chou, K.C. Melting temperature of a selected area in CaO-MgO-Al_2O_3-SiO_2 slag system[J]. Advanced Materials Research, 2011, 194-196: 169-174.

15. Wen, G.H.; Sridhar, S.; Tang, P.; Qi, X.; Liu, Y. Development of fluoride-free mold powders for peritectic steel slab casting[J]. ISIJ International, 2007, 47(8): 1117-1125.

16. Lee, S.; Min, D. J. Viscous behavior of FeO-Bearing slag melts considering structure of slag[J]. Steel Research International, 2018, 89(8): 1800055.

17. Sohn, I.; Min, D.J. A review of the relationship between viscosity and the structure of calcium-silicate-based slags in ironmaking[J]. Steel Research International, 2012, 83(7): 611-630.

18. Fu, G.Q.; Ju, H.X.; Xue, X.; Sun, J.; Wang, C.Y.; Zhu, M.Y. Study on Viscosity and Temperature of Acidic

402   Vanadium-titanium-containing Slag[J]. The Chinese Journal of Process Engineering, 2008, 8(1): 276-279.

403   19.   Wen, Y.C.; Zhou, J.Z.; Yang, S.B.; Zhang, Y.D.; Tang, T.Y.; Xu, L.Z.; Luan, Q.S.; Dong, L.R.; Study of
404   melting properties of converter slag containing vanadium and titanium oxides[J]. Iron steel vanadium
405   titanium, 2001, 22(3): 32-36.

406   20.   Kondretiev, A.; Jak, E. Predicting coal ash slag flow characteristics(viscosity model for the
407   Al_2O_3-CaO-FeO-SiO_2, system)[J]. Fuel, 2001, 80(14): 1989-2000.

408   21.   Nicholls, P.; Reid, W.T. Viscosity of coal-ash slag[J]. Transactions of the ASME, 1944, 66: 83-97.

409   22.   Park, H.S.; Park, S.S.; Sohn, I. The viscous behavior of FeO_t-Al_2O_3-SiO_2 copper smelting slags[J].
410   Metallurgical & Materials Transactions B, 2011, 42(4): 692-699

411   23.   Song, W.J.; Sun, Y.M.; Wu, Y.Q.; Zhu, Z.B.; Koyama, S. Measurement and simulation of flow properties of
412   coal ash slag in coal gasification[J]. Aiche Journel, 2011, 57(3): 801-818.

413   24.   Fincham, C.J.B.; Richardson, F.D. The Behaviour of Sulphur in Silicate and Aluminate Melts[J].
414   Proceedings of the Royal Society A, 1954, 223(1152): 40-62.

415   25.   Park, H.; Park, J.Y.; Kim, G.H.; Sohn, I. Effect of TiO_2 on the Viscosity and Slag Structure in Blast Furnace
416   Type Slags[J]. Steel Research International, 2012, 83(2):150-156.

417   26.   Björkman, B.O.; Eriksson, G.; Rosén, E. A generalized approach to the flood-knapp structure based model
418   for binary liquid silicates: Application and update for the PbO-SiO_2 System[J]. Metallurgical Transactions
419   B, 1984, 15(3): 511-516.

420   27.   Park, J.H.; Rhee, P.C.-H. Ionic properties of oxygen in slag[J]. Journal of Noncrystalline Solids, 2001, 282(1):
421   7-14.

422   28.   Yamashita, Y.; Hayes, P. Analysis of XPS spectra of Fe^{2+} and Fe^{3+} ions in oxide materials[J]. Applied Surface
423   Science, 2008, 254(8): 2441-2449.

424   29.   Toop, G.W.; Samis, C.S. Some new ionic concepts of silicate slags[J]. Canadian Metallurgical Quarterly,
425   1962, 1(2): 129-152.